Comparison of Ion Cyclotron Wall Conditioning Discharges in Hydrogen and Helium in JET

Y. Kovtun[a,*], T. Wauters[b], D. Matveev[c], R. Bisson[d], I. Jepu[e], S. Brezinsek[c], I. Coffey[e], E. Delabie[e], A. Boboc[e], T. Dittmar[c], A. Hakola[f], P. Jacquet[e], K. Kirov[e], E. Lerche[g,e], J. Likonen[f], E. Litherland-Smith[e], T. Loarer[h], P. Lomas[e], C. Lowry[e], E. Pawelec[i], C. Perez von Thun[j], A. Meigs[e], M. Maslov[e], I. Monakhov[e], C. Noble[e], S. Silburn[e], H. Sun[e], D. Taylor[e], E. Tsitrone[h], A. Widdowson[e], H. Sheikh[e], D. Douai[h] and JET Contributors[k]

[a]Institute of Plasma Physics of the NSC "KIPT", Kharkiv, Ukraine

[b] ITER Organization, Route de Vinon-sur-Verdon, CS 90 046, 13067 St Paul Lez Durance Cedex, France ;

[c]Forschungszentrum Jülich GmbH, IEK-4, Jülich, Germany;

[d]Aix-Marseille Univ, CNRS, PIIM, Marseille, France;

[e]UKAEA, CCFE, Culham Science Centre, Abingdon, Oxon, OX14 3DB, UK;

[f]VTT, Espoo, Finland;

[g]LPP-ERM/KMS, TEC, Brussels, Belgium;

[h]CEA, IRFM, Saint Paul Lez Durance, France;

[i]Institute of Physics, Opole University, Opole, Poland;

[j]Institute of Plasma Physics and Laser Microfusion, Hery 23, 01-497 Warsaw, Poland;

[k]See the author list of 'Overview of JET results for optimising ITER operation' by J. Mailloux et al 2022 Nucl. Fusion 62 042026

Abstract

This paper explores the plasma parameters of helium and hydrogen Ion Cyclotron Wall Conditioning (ICWC) discharges performed in JET as part of a He/H fuelling changeover experiment. The conducted study shows that plasma with a higher density is formed in helium than in hydrogen. A distinct glow in the ion cyclotron resonance zone is observed throughout the discharge in He. In H-ICWC discharges, a lower radio-frequency coupling efficiency and coupled power was observed than in He-ICWC discharges. While the helium concentration decreased with the number of H-ICWC pulses and the same for hydrogen in He-ICWC, which is the intended result of the plasma wall interaction in the ICWC changeover procedure, the main features of hydrogen as well as the helium IC discharge do not change dramatically.

Keywords: wall conditioning, radio-frequency discharge, tokamak, plasma production, ion cyclotron
*Corresponding author. E-mail address: Ykovtun@kipt.kharkov.ua; kovtuny41@gmail.com (Yu.V. Kovtun).

1. Introduction

Wall conditioning is essential for the operation of tokamaks and stellarators, and thus for the advancement of magnetic confinement fusion research [1-3]. It is applied to overcome several problems. First, to decrease the flux of impurities from the first wall into the confinement volume and, accordingly, to decrease the radiation losses from the plasma. Control of the recycling of hydrogen fuel fluxes and, therefore, plasma density. Removal of tritium from plasma-facing materials for safety. Accelerating the transition from plasma tests with one element or isotope to another. Recovering vacuum conditions after events such as disruptions and vacuum leaks.

Wall conditioning includes various methods [1, 2]. One such method is the use of plasma produced by radio-frequency (RF) discharges of various frequency ranges, including the ion-cyclotron frequency range [1-4]. This method has been and is used on stellarators W7-AS [5], U-3M [6], U-2M [7], LHD [8] and tokamaks TEXTOR [9], ASDEX Upgrade [10], TORE SUPRA [11], EAST [12], HT-7 [13], KSTAR [14]. Ion Cyclotron Wall Conditioning (ICWC) is one of the developed methods for fuel removal at JET [3, 4, 15]. In future it is planned to use ICWC in the superconducting stellarator W7-X [16] and tokamaks DTT [17], ITER [18]. ICWC can use the same antennas as used for ion cyclotron resonance heating (ICRH) without requiring additional hardware. However, the approaches in implementing ICWC and ICRH are quite different. In ICRH methods, RF power is applied to an already made plasma. In ICWC, the discharge is produced and sustained by the RF antenna, with parameters appropriate for wall conditioning procedures. Initial conditions (pressure, magnetic field, etc.) must be selected favorable for RF breakdown as well as for subsequent power coupling in the steady conditioning plasma [19]. The plasma parameters of the ICWC discharge affect the efficiency of wall conditioning. Therefore, ICWC discharge analysis is necessary to optimize the wall conditioning procedure.

Previously, discharge production for ICWC in JET was analyzed for example in [reference missing]. However, the comparison and analysis of the ICWC discharge plasma parameters in different gas atmospheres has not been carried out before. In the present work, we compare the ICWC discharge parameters in hydrogen (H_2) and helium (He) atmospheres in JET under nearly identical conditions. The experiments were conducted to investigate the effect of He/H changeover with Be/W walls.

2. Experimental details

The scenario was as follows. The hydrogen ICWC discharges were preceded by helium tokamak plasma operations and one reference pulse in hydrogen. Similarly, the helium ICWC discharges in the subsequent sessions followed eight tokamak pulses in hydrogen and one reference pulse in helium [20]. First, the plasma discharges in a tokamak with ICRH in a hydrogen atmosphere. Next, there were ICWC discharges in hydrogen to reduce the helium concentration in the facility. Then plasma discharges in a tokamak with ICRH in a hydrogen atmosphere. After that ICWC discharge in helium to decrease hydrogen concentration in the facility. And plasma discharges in a tokamak with ICRH in a helium atmosphere.

The ICRH system at JET includes one ITER-like antenna (ILA) and four A2 antennas known as the 'A', 'B', 'C', 'D' [21-24]. The latter A2 antennas have been used in ICWC experiments [25]. They each include four poloidal straps with a Faraday shield. Present experiment used antenna 'D' to produce the ICWC discharge plasma. The phasings of the antenna straps were 'monopole' (0 0 0 0). The generated RF power was up to 0.45 MW at a frequency of f_{RF} = 28.24 MHz. The toroidal magnetic field in the center was B_t = 1.9 T. In these conditions, the ion cyclotron resonance (ICR) zone for the fundamental harmonic of hydrogen ω_{ci} (H^+) ≈ $\omega_{RF} = 2\pi \times f_{RF}$ is localized on the torus axis ~ 3.04 m. At the same time, for He^{2+} and He^+ helium ions, the ICR zone for the first harmonic is outside the plasma volume. Correspondingly, for helium ions $\omega_{RF} \approx 2\omega_{ci}$ (He^{2+}) ≈ $4\omega_{ci}$ (He^+). In ICWC discharges in hydrogen there was additionally a shaped vertical magnetic field of magnitude 15 mT. In the two shots, #101044 and #101045 the value of the vertical field was 22.5 and 7.5 mT, respectively. Only four ICWC discharges in helium additionally had a vertical magnetic field 22.5 mT (#101082), 7.5 mT (#101083) and 15 mT (#101084, #101085).

The line integrated density was measured using a multi-channel Far Infrared (FIR) interferometer [26, 27] on four vertical channels (see Fig. 1a), with a sensitivity of 3×10^{17} m^{-2}. Time-resolved optical emission spectroscopy was used to measure the intensities of spectral lines of helium and hydrogen, as well as lines of plasma impurities. In the visible range, the spectrometric systems known as KS3 and KS8 [28] in JET were used. The poloidal cross section of the KS3 and KS8 viewing geometry is shown in Fig. 1b and Fig. 1c, respectively. The evolution of the ICWC discharge was registered by tangential video diagnostics. Residual gases were analyzed by sub-divertor gas analysis diagnostic [29, 30]. The sub-divertor hydrogen concentration was measured by Penning gauge spectroscopy [29, 30].

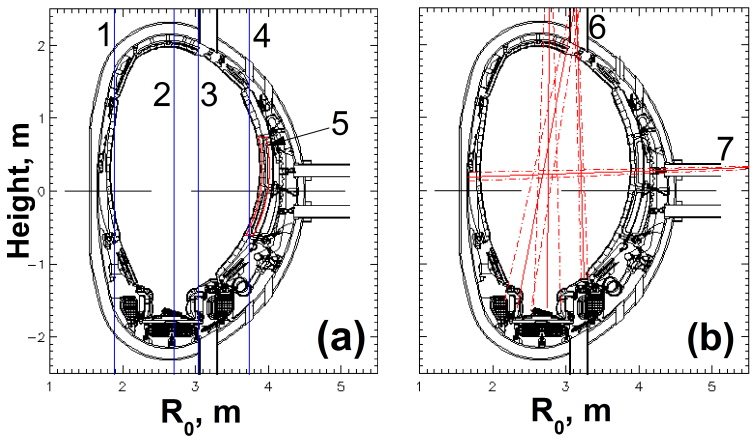

Fig.1. Poloidal cross section of the FIR (a) and spectrometer systems KS3 (b) viewing geometry. 1-4 vertical channels FIR, respectively, LID 1-LID 4; 5 - A2 antenna; 6 and 7 vertical and horizontal view KS3.

3. Results and discussion

The ICWC pulse starts by injecting RF power at ≈ 42.8 s, followed by gas injection The pulse injection of the operating gas was performed with a short time delay of ~ 400 ms, until relative to the start of the RF generator. ≈ 61.9 s, when both RF and gas stop. The time of the appearance of a plasma glow in the volume, recorded by a tangential high-speed video camera with a time resolution of 5 ms, was different for ICWC discharges in hydrogen and helium. In H-ICWC discharges, the glow appeared in the interval from ~ 0.3 to ~ 0.8 s after the start of gas filling. At the same time in He-ICWC discharges this time was from ~ 1 to ~ 2 s. In fact, during this time several processes take place sequentially. Reaching the pressure, concentration of neutral atoms, in the volume necessary for RF breakdown. The pressure of hydrogen and helium in the vacuum vessel at the start of the glow were ~ $(1.7\text{-}3)\times10^{-5}$ mbar and $(0.9\text{-}1.7)\times10^{-4}$ mbar, respectively. Breakdown and creation of a low-density plasma [19, 31], the glow of which can be registered by video diagnostics. The further dynamics of ICWC discharge glow is also different in hydrogen and helium. In H-ICWC discharges the brightest glow near the wall, the intensity of which varies over time (see fig. 2a,b). Shortly after the discharge initiation in He, the presence of horizontal filaments near the low field side was observed (see fig. 2c), suggesting that initially, the plasma flows from a localised plasma production zone along the shaped vertical magnetic field configuration. Also, a more intense glow in the ICR zone throughout the discharge in He is observed (see fig. 2d). Video diagnosis with the H_α filter (656 nm) shows an intense glow of the hydrogen line in the ICR region. Both features are not observed in H (see fig. 2a,b). The presence of a minority addition of hydrogen in the He-ICWC discharges is confirmed by both spectrometric diagnostics and Penning gauge spectroscopy.

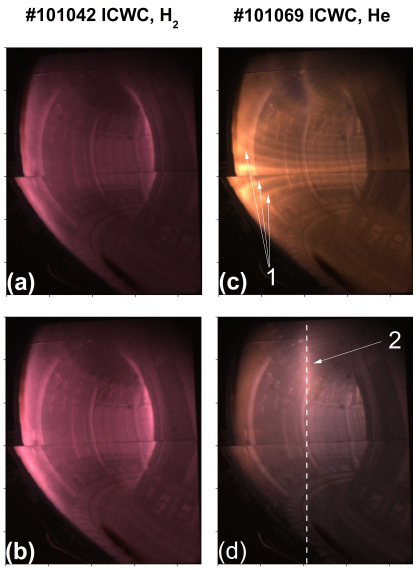

Fig. 2. Tangential camera images of a ICWC discharge in H_2 (a,b) and He (c, d). Time discharge 45.9 s (a, c) and 47.6 s (b,d). 1 - horizontal filaments, 2 - emission in ICR zone. Dash line approximate position ICR zone.

In Fig. 3 shows a comparison of the discharge parameters for two pulses in hydrogen and helium. As can be seen in both pulses there are spectral lines of hydrogen and helium. Accordingly, this shows the presence of the minority hydrogen or helium resulting from plasma wall interaction in addition to the main fuelled species. The highest intensity is observed for the spectral lines of the main gas. Significant differences are observed in the achieved plasma density for these discharges. Measurements of the line-integrated electron density along the vertical chord in the H-ICWC discharge showed that the density is below the accuracy of the interferometer of 3×10^{17} m^{-2}. In the case of the ICWC discharge in He, the density was higher than 3×10^{17} m^{-2}. The line-integrated electron density measurements (see fig. 3 a, c) were made in vertical channels LID 3 (see fig. 1a) at the radial coordinate $R_0 \approx 3.02$ m, which is very close to the ICR zone ~ 3.04 m. Correspondingly, the ICR zone also showed an increase in plasma density. The maximum achieved N_eL value was up to 6×10^{17} m^{-2}. The average density estimate gives a value of ~ 2×10^{17} m^{-3}. Higher densities are also observed in the other vertical channels LID 2 ($R_0 \approx 2.69$ m) and LID 4 ($R_0 \approx 3.75$ m) in the He-ICWC discharge. For LID 2 the maximum N_eL was up to 5.3×10^{17} m^{-2}, LID 4 was slightly above the interferometer sensitivity up to 3.2×10^{17} m^{-2}. Accordingly, the entire plasma volume has a higher density in He-ICWC than in H-ICWC discharges.

Fig. 3b,d shows the time evolution of the intensity of the spectral lines of hydrogen, helium, and impurities in the vertical midplane. Just as in the horizontal midplane (see fig. 3a,c), the maximum intensity is observed for the spectral lines of the main gas and lower intensity for the

minority additive. In the He-ICWC discharge spectral lines of helium, oxygen, and carbon ions are also observed (see Fig. 3b,d). In H-ICWC discharge the spectral lines of helium and carbon ions are absent. The intensity of the oxygen spectral line is an order of magnitude lower than in the He-ICWC discharge. This difference may be directly due to the higher plasma density in the helium discharge and hence increased ionization and excitation collision rates, assuming identical plasma temperatures. Or indirect by an increased flux of particles both helium and including hydrogen [32] on the wall will increase and accordingly via plasma-wall interaction, an increased influx of impurities in the plasma. Accordingly the intensity of spectral lines of ions should increase. On the other hand it is also possible that the temperature of electrons in the helium discharge is higher than in hydrogen.

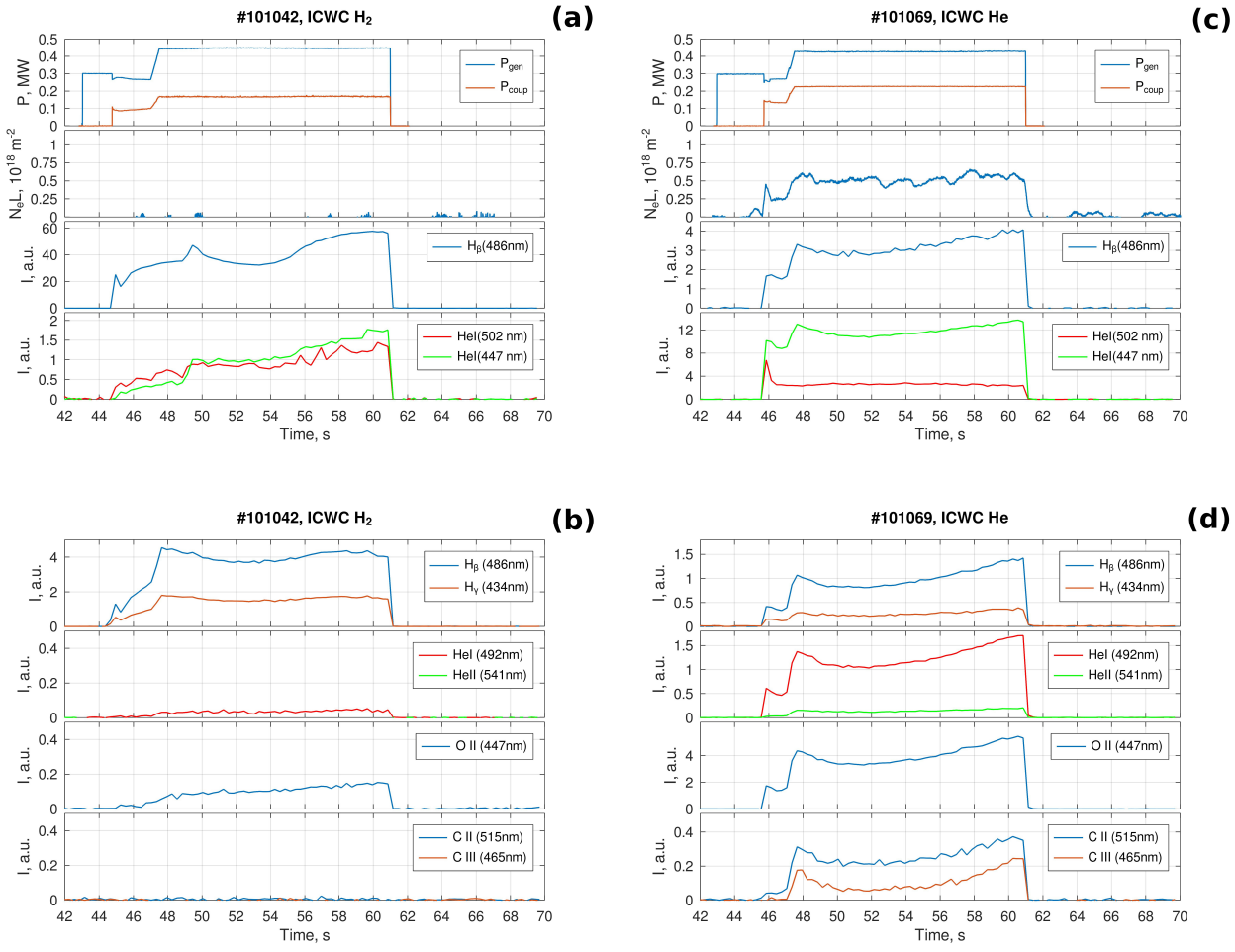

Fig.3. (a, c) Time evolutions of generated P_{gen} and coupled P_{coup} powers, line integrated electron density N_eL (LID 3, see fig.1a), optical emission intensities of H I and He I (horizontal midplane, KS 3, see fig. 1 b).

(b, d) Time evolutions of optical emission intensities of H I, He I and He II, O II, C II, C III (vertical, inner divertor, KS 3 see fig. 1 b). The ICWC discharge in H_2 (left), the ICWC discharge in He (right).

A difference in coupled RF power for ICWC discharge in hydrogen and helium is also observed (see fig. 3). Fig. 4 summarizes the RF parameters and line-integrated electron density for ICWC pulses. The efficiency of inputting RF power into the plasma is characterized by coupling efficiency η. The antenna–plasma coupling efficiency is the fraction of the power coupled to the plasma to the power launched at the generator, $\eta = P_{coup}/P_{gen}$ [19]. In H-ICWC discharges, a lower η was observed than in He-ICWC discharges, respectively up to 0.4 and 0.58. Accordingly, the coupled RF power P_{coup} in the H discharge was lower than in the He discharge, up to up to 0.16 MW and 0.24 MW respectively. The total coupled energy W_c in the H discharge was lower than in the He discharge, up to up to 1.2 MJ and 4 MJ respectively. Higher values of coupling efficiency, respectively P_{coup} and W_c in He-ICWC seem to be associated with a higher plasma density in the volume and other plasma parameters other than H-ICWC discharge. As a result, the coupling of the antenna to the plasma is higher.

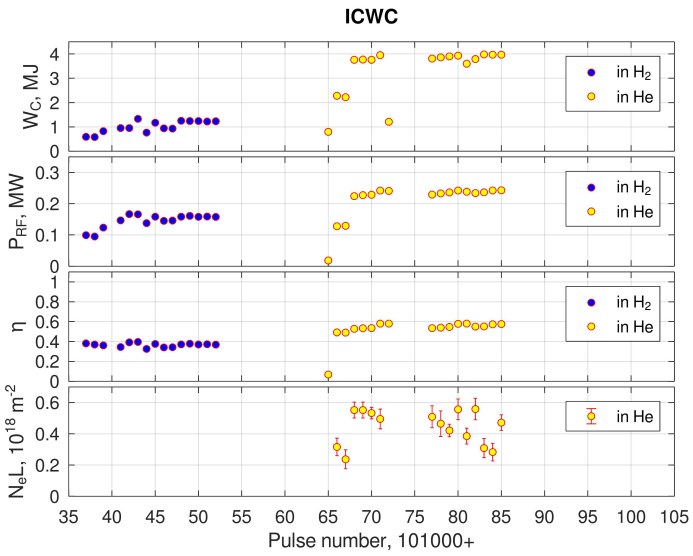

Fig. 4. The total coupled energy W_c, the average value at the time interval 50-55s coupled power P_{coup}, coupling efficiency η, line integrated electron density N_eL (LID 3, see fig.1a).

Fig. 5 shows the change in pressure and mass spectra during and after the RF pulse. As can be seen, both the hydrogen and helium pressure increases after the RF pulse. The H-ICWC discharge also shows an increase in the signal on the mass spectrum not only for H_2 (m = 2) but also for He (m = 4), HD (m = 3), and H_2O (m = 18). The situation after the He-ICWC discharge is different, where the signals increase only for He (m = 4) and H_2 (m = 2). Penning gauge spectroscopy show a helium concentration of ~ 3 - 9 % in the H-ICWC discharge and ~ 0.7 - 6 % of Hydrogen in the He-ICWC discharge. It is observed that the concentration of helium decreases with

the number of H-ICWC pulses and the same for hydrogen in He-ICWC. This is the result of the progressing He/H changeover via the interaction of plasma with the wall in the ICWC procedure.

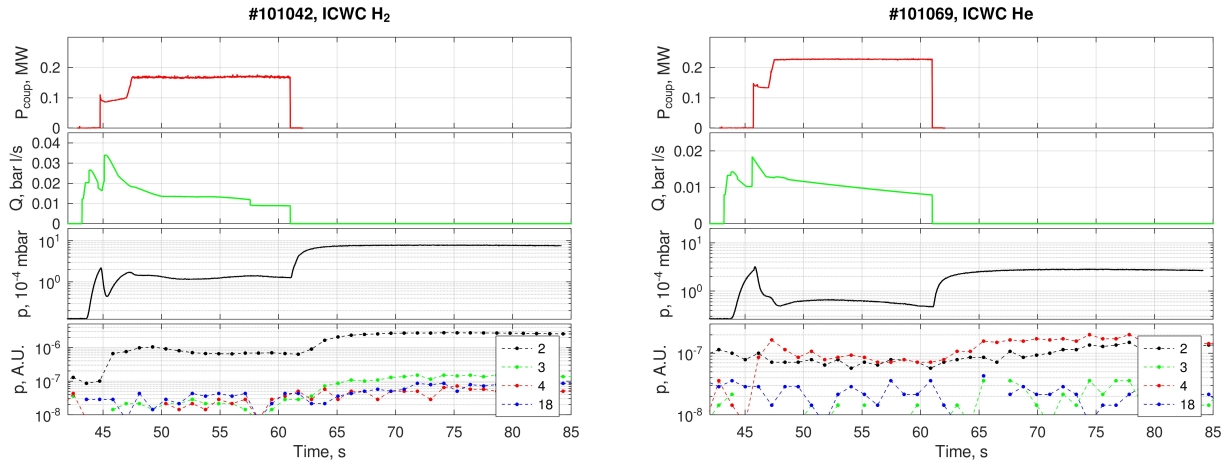

Fig. 5. Time evolutions of coupled power P_{coup}, gas flow rate Q, pressure p, mass spectrum. The ICWC discharge in H_2 (left), the ICWC discharge in He (right).

The differences in hydrogen and helium ICWC discharges in JET seem to be due to the presence of a hydrogen minority additive in helium. A similar results was also observed in D-ICWC with minority H_2 and H-ICWC with minority D_2 at JET. In both experiments, three antennas 'A', 'B', and 'D' at ≈ 25 MHz were used to produce plasma. In the D-ICWC experiments with minority H_2 the toroidal magnetic field was ≈ 1.65 T and, accordingly, the condition $\omega_{RF} \approx \omega_{ci}$ (H^+) ≈ $2\omega_{ci}$ (D^+) was satisfied. The hydrogen concentration in the D-ICWC was ~3-9%. In H-ICWC experiments with minority D_2 the magnetic field value was $B_t \approx 3.3$ T and, accordingly, $\omega_{RF} \approx \omega_{ci}$ (D^+), ω_{ci} (H^+) > ω_{RF}. The deuterium concentration was ~ 8-9%. In both experiments, a glow was observed in the ICR zone, as can be seen in Fig. 6. As well as a higher plasma density in this region. Thus, in D-ICWC with minority H_2 in some pulses the density reached the value $N_eL \approx 2.7\times10^{18}$ m^{-2} (LID 3), while in H-ICWC discharges with minority D_2 densities up to 7.4×10^{18} m^{-2} (LID 3) have been achieved.

A similar situation is observed in studies of ICRF plasma production with minor additions of hydrogen in helium on Uragan-2M and LHD stellarators [33-37]. In the case of minor additions of H_2 in He, the plasma density was higher than in pure hydrogen or helium [35, 37]. These differences are explained by the intense heating of the plasma electrons in the mode conversion regime [33]. The results in JET in ICWC discharges with minority additives can be ascribed to the same process.

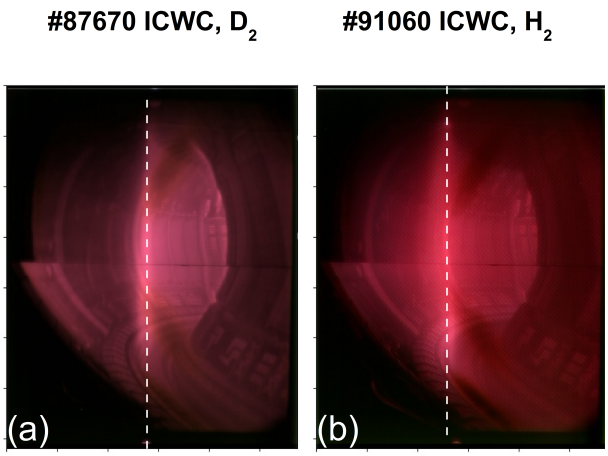

Fig. 6. Tangential camera images of a D-ICWC discharge with minority H_2 (a) and H-ICWC discharge with minority D_2. Time discharge 45.6 s (a, b). Dash line approximate position ICR zone.

4. Conclusions

This paper explores the plasma and discharge parameters of helium and hydrogen ICWC discharges at JET. The conducted studies of the ICWC discharge show that plasma with a higher density is formed in helium up to 6×10^{17} m^{-2}, respectively ~ 2×10^{17} m^{-3}, than in hydrogen. Shortly after the discharge initiation in He, the presence of horizontal filaments near the low field side was observed. This indicates that the plasma initially flows from a localized plasma production zone along the barrel shaped configuration of the magnetic field. A more intense glow in the visible range and the hydrogen H_α line in the ICR area throughout the discharge in He is observed. Both features are not observed in H. In H-ICWC discharges, a lower RF coupling efficiency was observed than in He-ICWC discharges, respectively up to 0.4 and 0.58. Accordingly, the coupled RF power in the H discharge was lower than in the He discharge, up to up to 0.16 MW and 0.24 MW respectively. Higher values of coupling efficiency seem to be associated with a higher plasma density in the volume. The difference in ICWC discharges in hydrogen and helium on JET seems to be due to the presence of hydrogen minority additive in helium, and the related possible heating of the plasma electrons in the mode conversion regime.

It is observed that the concentration of helium decreases with the number of H-ICWC pulses and per turn of hydrogen in He-ICWC. Which is the result of He/H changeover in the interaction of plasma with the wall in the ICWC procedure. These results will serve to optimize the wall conditioning procedure and develop an ICWC strategy for superconducting devices.

Acknowledgements

This work has been carried out within the framework of the EUROfusion Consortium, funded by the European Union via the Euratom Research and Training Programme (Grant Agreement No 101052200 — EUROfusion). Views and opinions expressed are however those of the author(s) only and do not necessarily reflect those of the European Union or the European Commission. Neither the European Union nor the European Commission can be held responsible for them.

This scientific paper has been published as part of the international project co-financed by the Polish Ministry of Science and Higher Education within the programme called 'PMW' for 2022-2023.

The views and opinions expressed herein do not necessarily reflect those of the ITER Organization.

References

1. J. Winter, Wall conditioning in fusion devices and its influence on plasma performance, Plasma Phys. Control. Fusion, 38 (1996) 1503–42 https://doi.org/10.1088/0741-3335/38/9/001

2. T. Wauters, D. Borodin, R. Brakel, et al., Wall conditioning in fusion devices with superconducting coils, Plasma Phys. Control. Fusion 62 (2020) 034002 https://doi.org/10.1088/1361-6587/ab5ad0

3. D. Douai, A. Lyssoivan, V. Philipps et al., Recent results on Ion Cyclotron Wall Conditioning in mid and large size tokamaks, J. Nucl. Mater. 415 (2011) S1021 https://doi.org/10.1016/j.jnucmat.2010.11.083

4. E de la Cal and E Gauthier, Review of radio frequency conditioning discharges with magnetic fields in superconducting fusion reactors, Plasma Phys. Control. Fusion 47 (2005) 197 https://doi.org/10.1088/0741-3335/47/2/001

5. R. Brakel, D. Hartmann, P. Grigull, ICRF wall conditioning experiments in the W7-AS stellarator, J. Nucl. Mater. 290–293 (2001) 1160-1164 https://doi.org/10.1016/S0022-3115(00)00554-7

6. A.V. Lozin, V. E. Moiseenko, L. I. Grigor’eva, et al., Cleaning of inner vacuum surfaces in the Uragan-3M facility by radio-frequency discharges, Plasma Phys. Rep. 39 (2013) 624-631. https://doi.org/10.1134/S1063780X13070052

7. Yu. V. Kovtun, V. E. Moiseenko, A. V. Lozin et al., Radio frequency wall conditioning discharges at low magnetic fields in Uragan-2M stellarator, 48th EPS Conference on Plasma Physics, 27 June - 1 July 2022, Online, Maastricht, Netherlands, ECA Vol. 46A, O2.J503.

8. M. Tanaka, H. Kato, N. Suzuki, et al., Removal of tritium from vacuum vessel by RF heated plasmas in LHD, Phys. Scr. 96 (2021) 124007 https://doi.org/10.1088/1402-4896/ac1bf2

9. H.G. Esser, A. Lyssoivan, M. Freisinger, et al., ICRF wall conditioning at TEXTOR-94 in the presence of a 2.25 T magnetic field, J. Nucl. Mater. 241-243 (1997) 861-866 https://doi.org/10.1016/S0022-3115(97)80155-9

10. A. Hakola, S. Brezinsek, D. Douai, et al., Plasma-wall interaction studies in the full-W ASDEX upgrade during helium plasma discharges, Nucl. Fusion 57 (2017) 066015 https://doi.org/10.1088/1741-4326/aa69c4

11. E. Gauthier, E. de la Cal, B. Beaumont, et al., Wall conditioning technique development in Tore Supra with permanent magnetic field by ICRF wave injection, J. Nucl. Mater. 241–243 (1997) 553-558 https://doi.org/10.1016/S0022-3115(97)80098-0

12. Yu. Yaowei, Jiansheng Hu, Yanping Zhao, et al., ICRF (ion cyclotron range of frequencies) discharge cleaning with toroidal and vertical fields on EAST, Plasma Phys. Control. Fusion 53 (2011) 015013 https://doi.org/10.1088/0741-3335/53/1/015013

13. J.S. Hu, J.G. Li, Y.P. Zhao He–ICR cleanings on full metallic walls in EAST full superconducting tokamak, J. Nucl. Mater. 376 (2008) 207–210 https://doi.org/10.1016/j.jnucmat.2008.02.090

14. Dong Su Lee, Suk-Ho Hong, Sungwoo Kim, et al., Ion Cyclotron Wall Conditioning (ICWC) on KSTAR, Fusion Eng. Des. 60 (2011) 94-97 https://doi.org/10.13182/FST11-A12412

15. T. Wauters, D. Matveev, D. Douai et al., Isotope removal experiment in JET-ILW in view of T-removal after the 2nd DT campaign at JET, Phys. Scr. 97 (2022) 044001 https://doi.org/10.1088/1402-4896/ac5856

16. J. Ongena, D. Castano-Bardawil, K. Cromb´e, et al., Physics design, construction and commissioning of the ICRH system for the stellarator Wendelstein 7-X, Fusion Eng. Des. 192 (2023) 113627 https://doi.org/10.1016/j.fusengdes.2023.113627

17. G.L. Ravera, S. Ceccuzzi, G. Granucci, et al., Operational requirements of the ion cyclotron wall conditioning in DTT, Fusion Eng. Des. 191 (2023) 113754 https://doi.org/10.1016/j.fusengdes.2023.113754

18. D. Douai, D. Kogut, T. Wauters, et al., Wall conditioning for ITER: Current experimental and modeling activities, J. Nucl. Mater. 463 (2015) 150–156 http://dx.doi.org/10.1016/j.jnucmat.2014.12.034

19. A. Lyssoivan, D. Douai, R. Koch et al., Simulation of ITER full-field ICWC scenario in JET: RF physics aspects, Plasma Phys. Control. Fusion 54 (2012), 074014 http://dx.doi.org/10.1088/0741-3335/54/7/074014

20. T. Wauters, R. Bisson, E. Delabie, et al., Changeover between helium and hydrogen fuelled plasmas in JET and WEST. Nuclear Martials and Energy (in press).
21. A. Kaye, T. Brown, V. Bhatnagar et al., Present and future JET ICRF antennae, Fusion Eng. Des. 24 (1994) 1-21 https://doi.org/10.1016/0920-3796(94)90034-5
22. M. Vrancken, M.-L. Mayoral, T. Blackman, Recent ICRF developments at JET, Fusion Eng. Des. 82 (2007) 873–880 https://doi.org/10.1016/j.fusengdes.2007.05.019
23. A Czarnecka, F. Durodie´, A. C. A. Figueiredo, et al., Plasma Phys. Control. Fusion 54 (2012) 074013 https://doi.org/10.1088/0741-3335/54/7/074013
24. I. Monakhov, P. Jacquet, T. Blackman, et al., ICRH antenna S-matrix measurements and plasma coupling characterisation at JET, Nucl. Fusion 58 (2018) 046012 https://doi.org/10.1088/1741-4326/aaace3
25. M. K. Paul, A. Lyssoivan, R. Koch et al., Plasma and antenna coupling characterization in ICRF-wall conditioning experiments, Fusion Eng. Des. 87 (2012) 98–103 https://doi.org/10.1016/j.fusengdes.2011.10.009
26. A. Boboc, C. Gil, P. Pastor, et al., Upgrade of the JET far infrared interferometer diagnostica, Rev. Sci. Instrum. 83 (2012) 10E341 http://dx.doi.org/10.1063/1.4737420
27. A. Boboc, B. Bieg, R. Felton, et al., A novel calibration method for the JET real-time far infrared polarimeter and integration of polarimetry-based line-integrated density measurements for machine protection of a fusion plant, Rev. Sci. Instrum. 86 (2015) 091301 https://doi.org/10.1063/1.4929443
28. C. F. Maggi, S. Brezinsek, M. F. Stamp, et al., A new visible spectroscopy diagnostic for the JET ITER-like wall main chambera, Rev. Sci. Instrum. 83 (2012) 10D517 http://dx.doi.org/10.1063/1.4733734
29. U. Kruezi, G. Sergienko, P. D. Morgan, et al., JET divertor diagnostic upgrade for neutral gas analysis, Rev. Sci. Instrum. 83 (2012) 10D728 https://doi.org/10.1063/1.4732175
30. U. Kruezi, I. Jepu, G. Sergienko, et al., JINST 15 (2020) C01032 https://doi.org/10.1088/1748-0221/15/01/C01032
31. M. Tripský, T. Wauters, A. Lyssoivan et al., A PIC-MCC code RFdinity1d for simulation of discharge initiation by ICRF antenna, Nucl. Fusion 57 (2017) 126043. https://doi.org/10.1088/1741-4326/aa8446
32. T. Wauters, A. Lyssoivan, D Douai et al., 0D model of magnetized hydrogen–helium wall conditioning plasmas, Plasma Phys. Control. Fusion 53 (2011) 125003. https://doi.org/10.1088/0741-3335/53/12/125003

33. V. Moiseenko, Yu. V. Kovtun, T. Wauters et al., First experiments on ICRF discharge generation by a W7-X-like antenna in the Uragan-2M stellarator, J. Plasma Phys., 86 (2020) 905860517. https://doi.org/10.1017/S0022377820001099

34. S. Kamio, V.E. Moiseenko, Yu.V. Kovtun et al., First experiments on plasma production using field-aligned ICRF fast wave antennas in the large helical device, Nucl. Fusion. 61 (2021) 114004. https://doi.org/10.1088/1741-4326/ac277b

35. V. Moiseenko, Yu. V. Kovtun, A. V. Lozin et al., Plasma Production in ICRF in the Uragan-2M Stellarator in Hydrogen–Helium Gas Mixture, Journal of Fusion Energy. 41 (2022) 15. https://doi.org/10.1007/s10894-022-00326-8

36. Yu. V. Kovtun, V. Moiseenko, A. V. Lozin et al., ICRF Plasma Production with the W7-X Like Antenna in the Uragan-2M Stellarator, Plasma Fusion Res. 17 (2022) 2402034. https://doi.org/10.1585/pfr.17.2402034

37. Y. V. Kovtun, V. E. Moiseenko, S. Kamio et al. ICRF Plasma Production with Hydrogen Minority Heating in Uragan-2M and Large Helical Device. Plasma Fusion Res. 18, (2023) 2402042 https://doi.org/10.1585/pfr.18.2402042